Star Formation Newsletter No. 339, 25-32

植田 高啓 (国立天文台)

25. Molecular Clouds in the Second Quadrant of the Milky Way Mid-plane from l=104.75 to l=119.75 and b=−5.25 to b=5.25

26. The Galactic HII Region Luminosity Function at Radio and Infrared Wavelengths

27. Gravitoviscous protoplanetary disks with a dust component. V. The dynamic model for freeze-out and sublimation of volatiles

28. Dipper-like variability of the Gaia alerted young star V555 Ori

29. OMC-1 dust polarisation in ALMA Band 7: Diagnosing grain alignment mechanisms in the vicinity of Orion Source I

30. The substructure of the Perseus star forming region: A survey with Gaia DR2

31. Detection of new O-type stars in the obscured stellar cluster Tr 16-SE in the Carina Nebula with KMOS

32. A Galactic survey of radio jets from massive protostars

29. **OMC-1 dust polarisation in ALMA Band 7: Diagnosing grain alignment mechanisms in the vicinity of Orion Source I**

Kate Pattle, Shih-Ping Lai, Melvyn Wright, Simon Coudé, Richard Plambeck, Thiem Hoang, Ya-Wen Tang, Pierre Bastien, Chakali Eswaraiah, Ray Furuya, Jihye Hwang, Shu-ichiro Inutsuka, Kee-Tae Kim, Florian Kirchschlager, Woojin Kwon, Chang Won Lee, Sheng-Yuan Liu, Aran Lyo, Nagayoshi Ohashi, Mark Rawlings, Mehrnoosh Tahani, Motohide Tamura, Archana Soam, Jia-Wei Wang, Derek Ward-Thompson

★ We present ALMA Band 7 polarisation observations of the OMC-1 region of the Orion molecular cloud. We find that the polarisation pattern observed in the region is likely to have been significantly altered by the radiation field of the $> 10^4$ $L_\odot$ high-mass protostar Orion Source I. In the protostar's optically thick disc, polarisation is likely to arise from dust self-scattering. In material to the south of Source I - previously identified as a region of 'anomalous' polarisation emission - we observe a polarisation geometry concentric around Source I. We demonstrate that Source I's extreme luminosity may be sufficient to make the radiative precession timescale shorter than the Larmor timescale for moderately large grains ($> 0.005 - 0.1\,\mu$m), causing them to precess around the radiation anisotropy vector (k-RATs) rather than the magnetic field direction (B-RATs). This requires relatively unobscured emission from Source I, supporting the hypothesis that emission in this region arises from the cavity wall of the Source I outflow. This is one of the first times that evidence for k-RAT alignment has been found outside of a protostellar disc or AGB star envelope. Alternatively, the grains may remain aligned by B-RATs and trace gas infall onto the Main Ridge. Elsewhere, we largely find the magnetic field geometry to be radial around the BN/KL explosion centre, consistent with previous observations. However, in the Main Ridge, the magnetic field geometry appears to remain consistent with the larger-scale magnetic field, perhaps indicative of the ability of the dense Ridge to resist disruption by the BN/KL explosion.

https://arxiv.org/abs/2009.14758

オリオン座分子雲の中心に位置する大質量星形成領域OMC-1のALMA Band 7 偏光観測。主に以下のことがわかった。

- 大質量星原子星Orion Source I 周りの円盤成分の偏光は自己散乱由来
- OMC-1の”the Fork”領域では、Orion Source Iからの輻射場に揃っている可能性がある
  （原始惑星系円盤/AGB星周りのエンベロープ以外ではじめて輻射場整列の可能性を示唆）
- 磁場整列の場合は、Orion Source Iを中心とする動径方向磁場に整列

観測領域まとめ

アウトフローをトレース

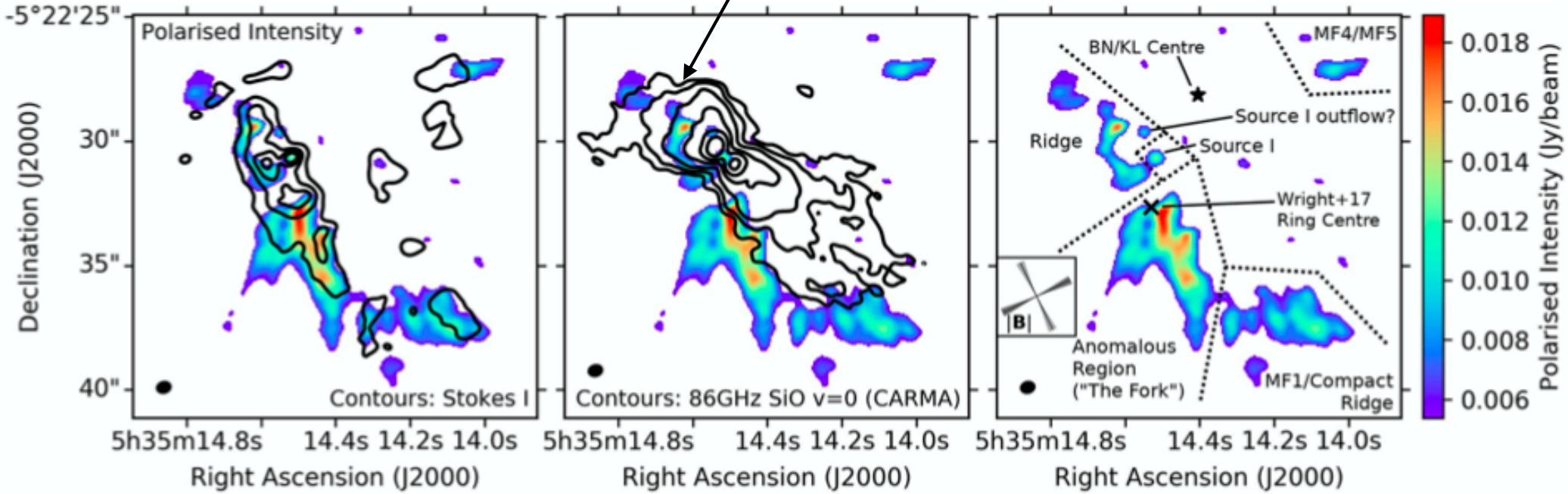

ISMでの偏光は磁場に整列したダストによって引き起こされると考えられるため、磁場構造を理解する上で役立つ。

OMC-1領域の偏光ベクトルは何に揃っているか？

1. 大局磁場（図左上から右下方向）
2. BN/KL centerを中心とした円
3. Source Iを中心とした円

-> ダスト整列メカニズムの制限/本当に磁場整列か？

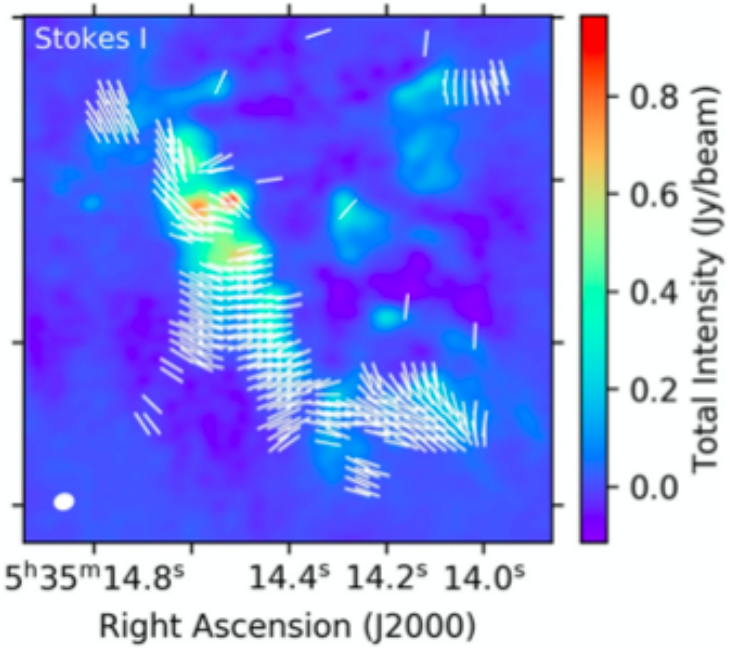

Source I 円盤の偏光：自己散乱由来が最も整合的（ただしBN/KL explosion 由来の整列も可）
-> ダストは少なくとも140um程度以上に成長している可能性
（Hirota+20でBand3の偏光度が<1%とされているので、ダストサイズは140-500um?）

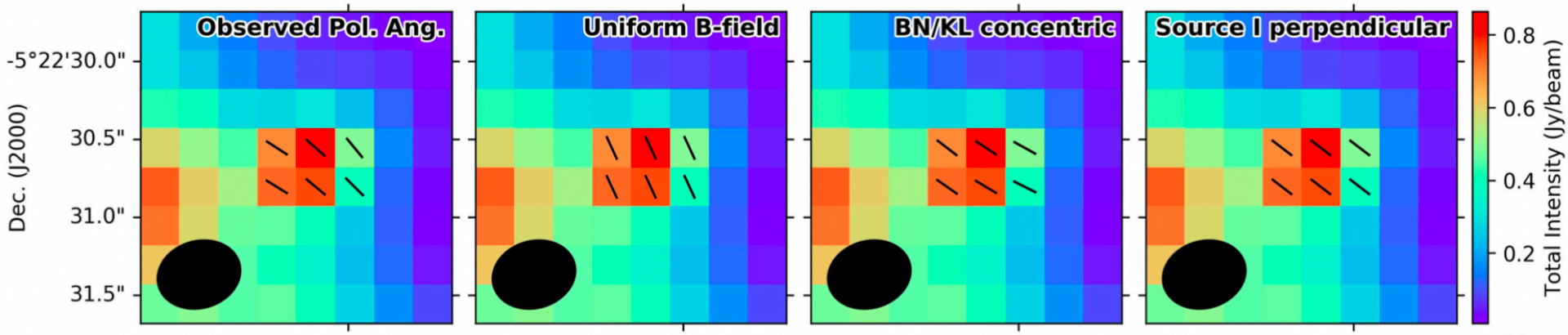

Anomalous Region (The Fork):

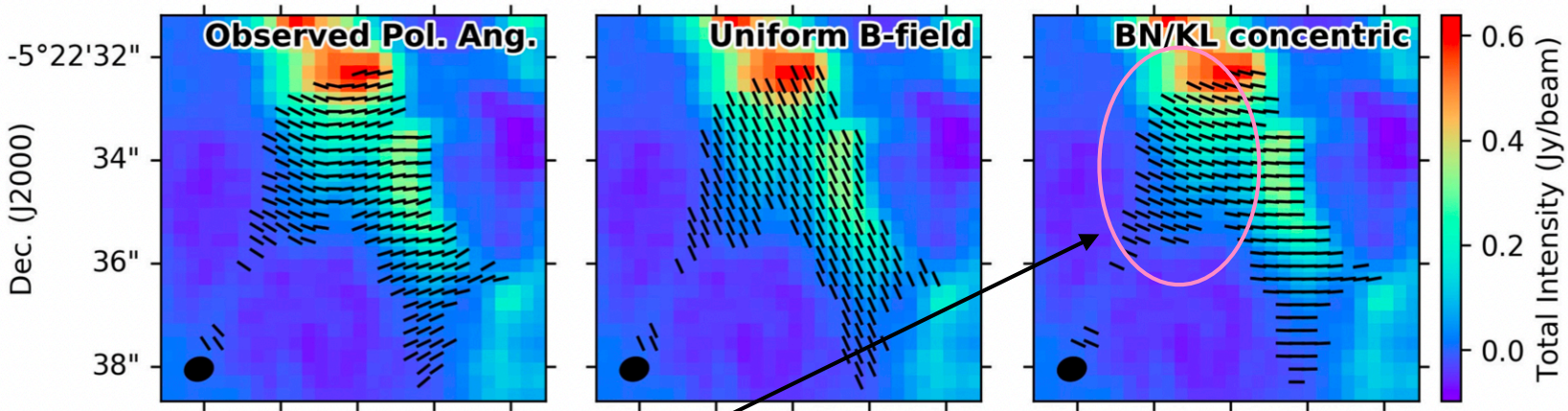

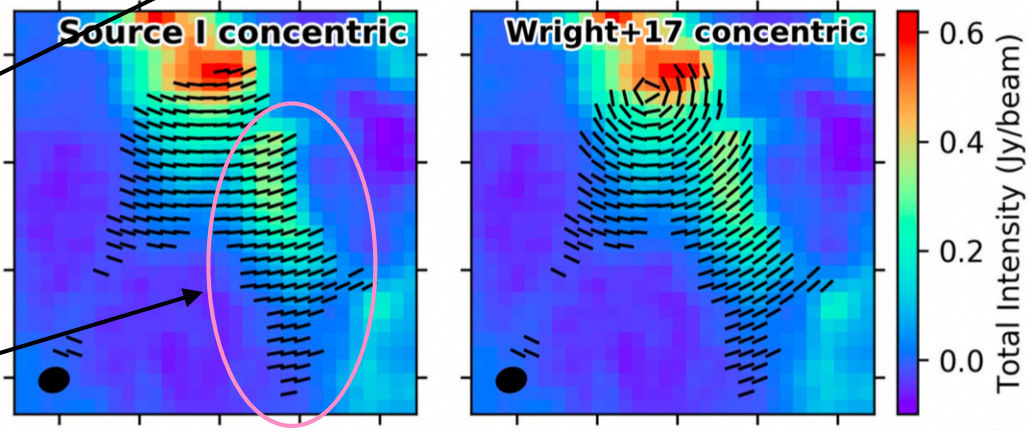

- 大局磁場には整列していない
- 東側はBN/KL concentric modelが整合的
  -> BN/KLを中心とした動径方向の磁場に整列(Cortes+21)
- 西側はSource I concentric modelが整合的

東側ではSource I を中心とした円に沿った偏光ベクトルを示しているが、何に整列しているのか？

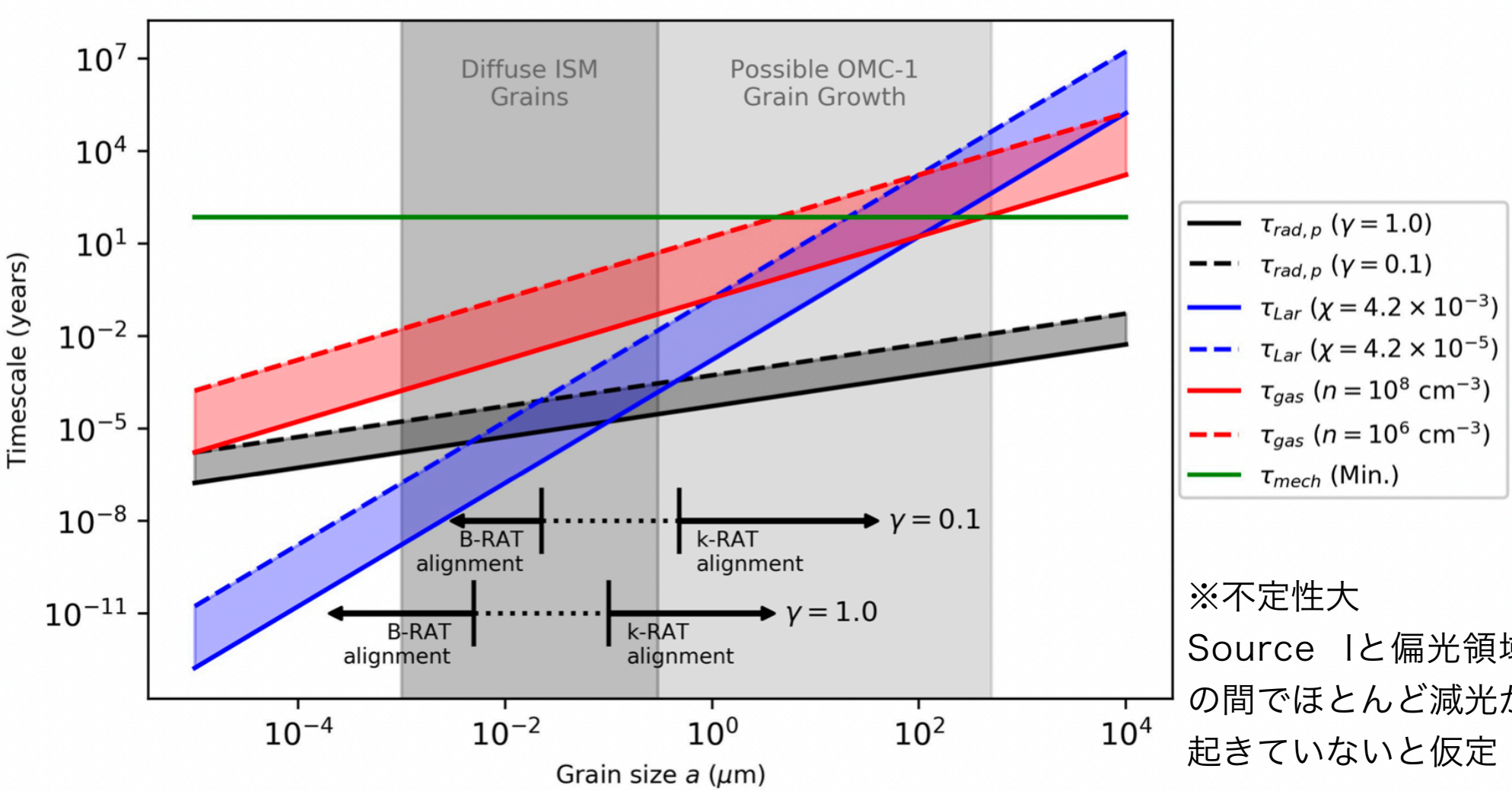

※不定性大
Source Iと偏光領域の間でほとんど減光が起きていないと仮定

- ダストが>0.1umの場合、Source Iからの輻射勾配に整列している
  ->大質量星が近くにある場合、ISMでも磁場でなく輻射場に整列している可能性がある
- ダストが<0.01umの場合、磁場に整列している
  -> 磁場整列の場合、大局磁場とは向きが異なるため、Source I のアウトフローによって磁場が大きく変化している

27. **Gravitoviscous protoplanetary disks with a dust component. V. The dynamic model for freeze-out and sublimation of volatiles**

Tamara Molyarova, Eduard I. Vorobyov, Vitaly Akimkin, Aleksandr Skliarevskii, Dmitri Wiebe, Manuel Güdel

★ The snowlines of various volatile species in protoplanetary disks are associated with abrupt changes in gas composition and dust physical properties. Volatiles may affect dust growth, as they cover grains with icy mantles that can change the fragmentation velocity of the grains. In turn, dust coagulation, fragmentation, and drift through the gas disk can contribute to the redistribution of volatiles between the ice and gas phases. Here we present the hydrodynamic model FEOSAD for protoplanetary disks with two dust populations and volatile dynamics. We compute the spatial distributions of major volatile molecules (H_2O, CO_2, CH_4, and CO) in the gas, on small and grown dust, and analyze the composition of icy mantles over the initial 0.5 Myr of disk evolution. We show that most of ice arrives to the grown dust through coagulation with small grains. Spiral structures and dust rings forming in the disk, as well as photodissociation in the outer regions, lead to the formation of complex snowline shapes and multiple snowlines for each volatile species. During the considered disk evolution, the snowlines shift closer to the star, with their final position being a factor $4-5$ smaller than that at the disk formation epoch. We demonstrate that volatiles tend to collect in the vicinity of their snowlines, both in the ice and gas phases, leading to the formation of thick icy mantles potentially important for dust dynamics. The dust size is affected by a lower fragmentation velocity of bare grains in the model with a higher turbulent viscosity.

https://arxiv.org/abs/2103.06045

原始惑星系円盤中の揮発性分子のスノーラインは、その分子が主に気相・固相のどちらにいるかを決める。揮発性分子が岩石ダスト表面に凝縮すると、ダストの付着効率が変化することでダストの成長にも影響を与える。本研究では、円盤形成の流体シミュレーションにダスト進化と揮発性分子の昇華・凝縮の効果を組み込むことで、円盤進化初期段階での揮発性分子の分布およびそのダスト進化への影響を調べた。その結果以下のことがわかった。

(1) 揮発性分子は主に、まず小さいダストへ凝縮し、そのダストが大きいダストに付着する
(2) 重力不安定スパイラルによる非軸対称スノーライン/光脱離による遠方スノーライン
(3) 進化初期のスノーラインの位置は後期の4-5倍外側
(4) 各揮発性分子の分布は、そのスノーライン近傍で気相・固相両方でピークをもつ

モチベーション

流体計算・ダスト進化・化学反応を同時に解くことで、円盤進化初期段階での揮発性分子の分布およびそのダスト進化への影響を見たい（と思われる）

モデル

- 流体計算コード FEOSAD (Vorobyov+18)を使った分子雲コア収縮からの円盤進化計算
- 簡単化したダスト成長

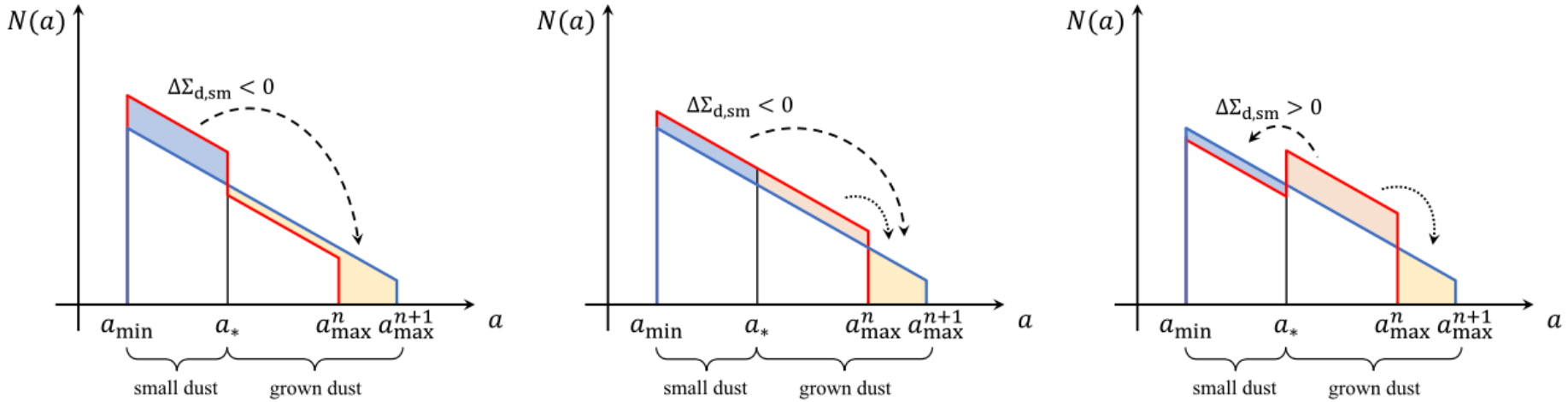

- H_2O, CO, CO_2, CH_4のダストへの吸着・熱脱離・光脱離

$$\frac{d\Sigma_s^{\rm gas}}{dt} = -\lambda_s \Sigma_s^{\rm gas} + \eta_s^{\rm sm} + \eta_s^{\rm gr},$$

$$\frac{d\Sigma_s^{\rm sm}}{dt} = \lambda_s^{\rm sm} \Sigma_s^{\rm gas} - \eta_{\rm sm}^{s},$$

$$\frac{d\Sigma_s^{\rm gr}}{dt} = \lambda_s^{\rm gr} \Sigma_s^{\rm gas} - \eta_s^{\rm gr},$$

- ice mantleがダスト成長に与える影響
  ice成分が一定量を超えると、付着効率UP

$$v_{\rm frag} = \begin{cases} 15\ {\rm m\ s^{-1}}, & {\rm if}\ \ \Sigma_{\rm ice}/\Sigma_{\rm d,gr} > K; \\ 1.5\ {\rm m\ s^{-1}}, & {\rm if}\ \ \Sigma_{\rm ice}/\Sigma_{\rm d,gr} \leqslant K. \end{cases}$$

K：ダストの表面を一様にiceが覆えるかどうかを表す変数

$\alpha=10^{-2}$

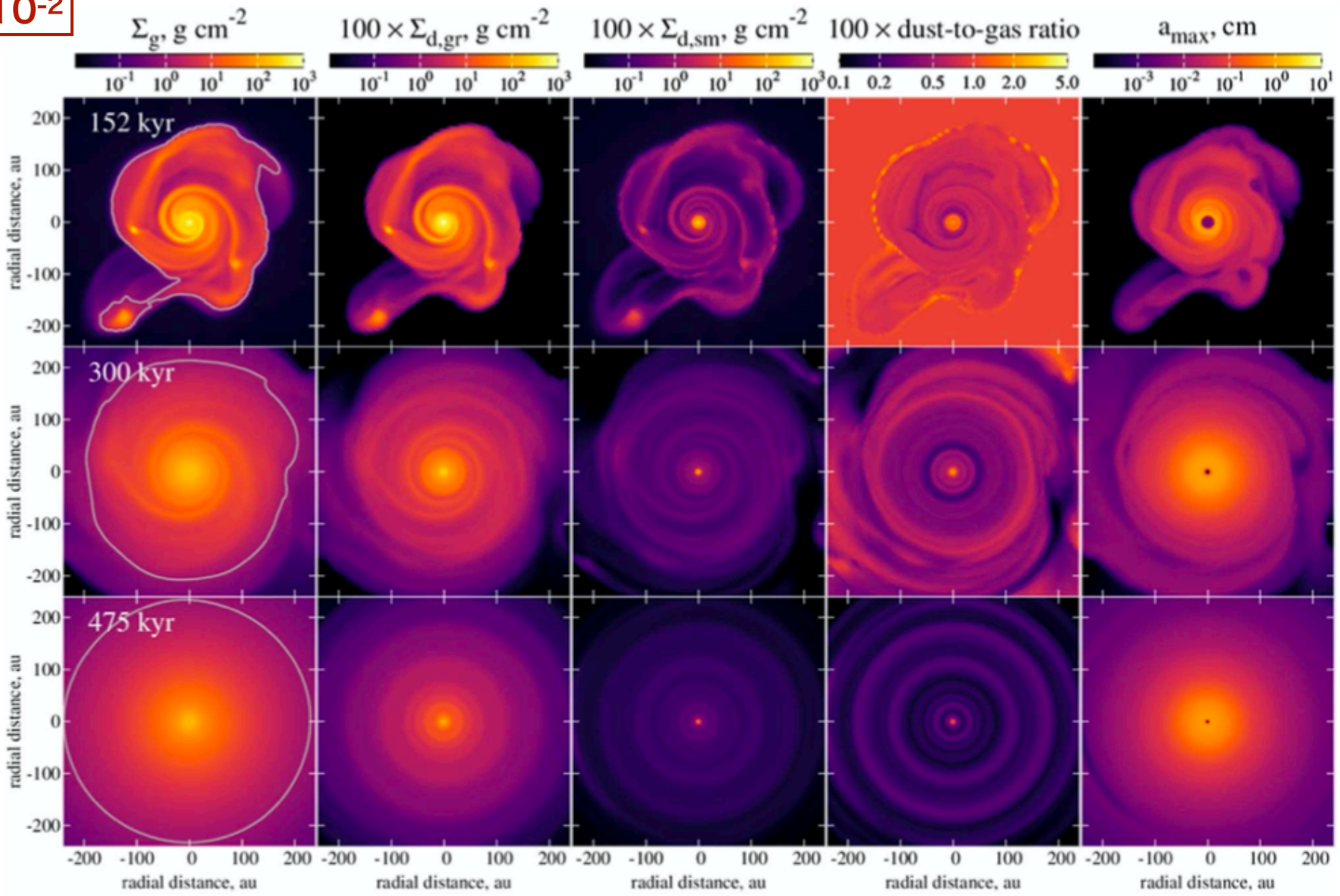

- 初期は重力不安定によるスパイラルができる。~475000年程度でほぼ軸対称。
- 成長したダストのドリフトによって、軸対称になるころにはダストガス比が<0.01
- 内側領域(5-20au)はiceに欠乏しているため、ダスト小さく高ダストガス比になる
- 後期はダストの多重リング構造が形成（後述）

$\alpha=10^{-4}$

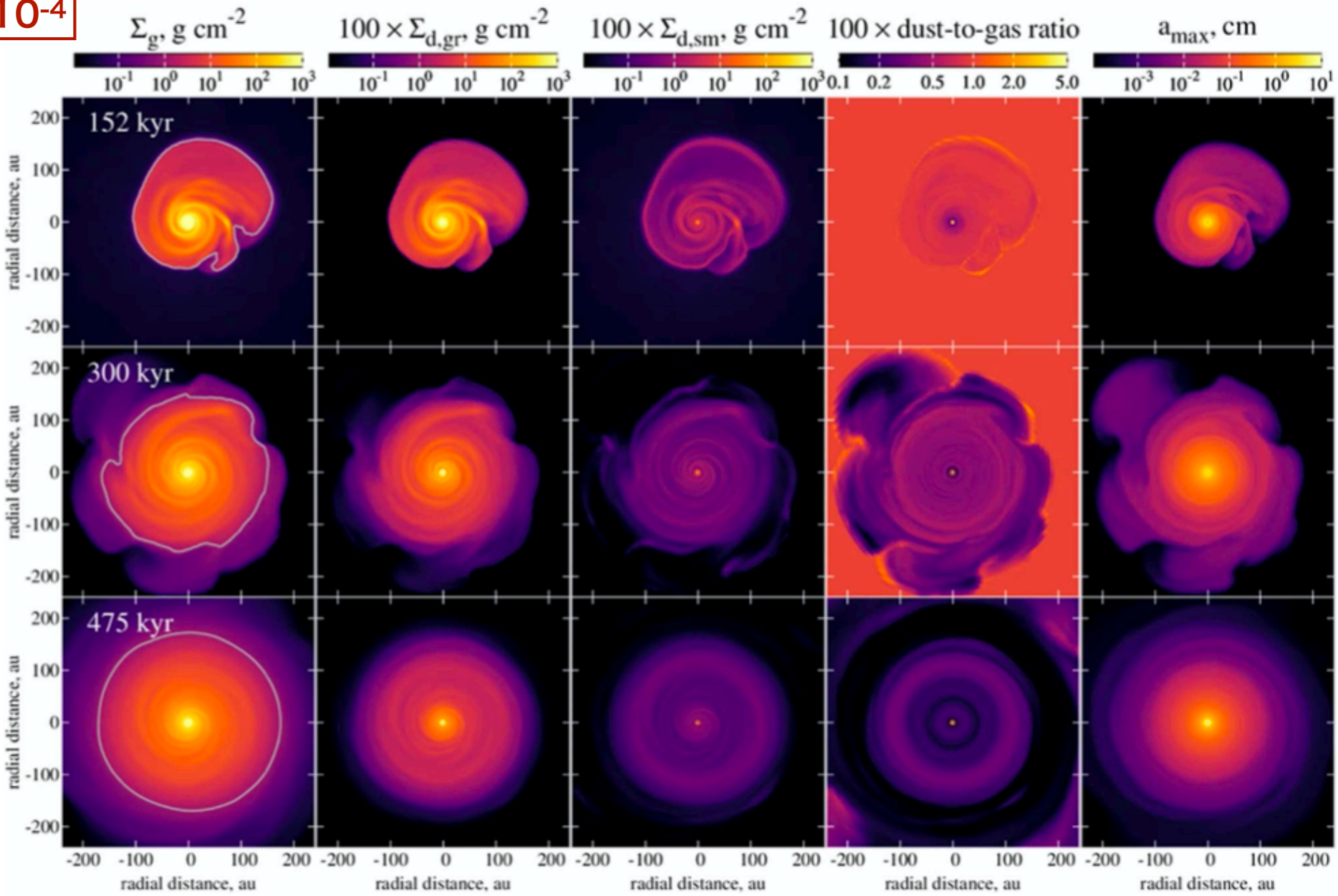

- $\alpha=10^{-4}$の場合、ガスが外に拡散しづらく、かつ温度も高くなるため、重力不安定によるクランプ形成が起きない

$\alpha=10^{-4}$

ガス　　大きいダスト　　小さいダスト

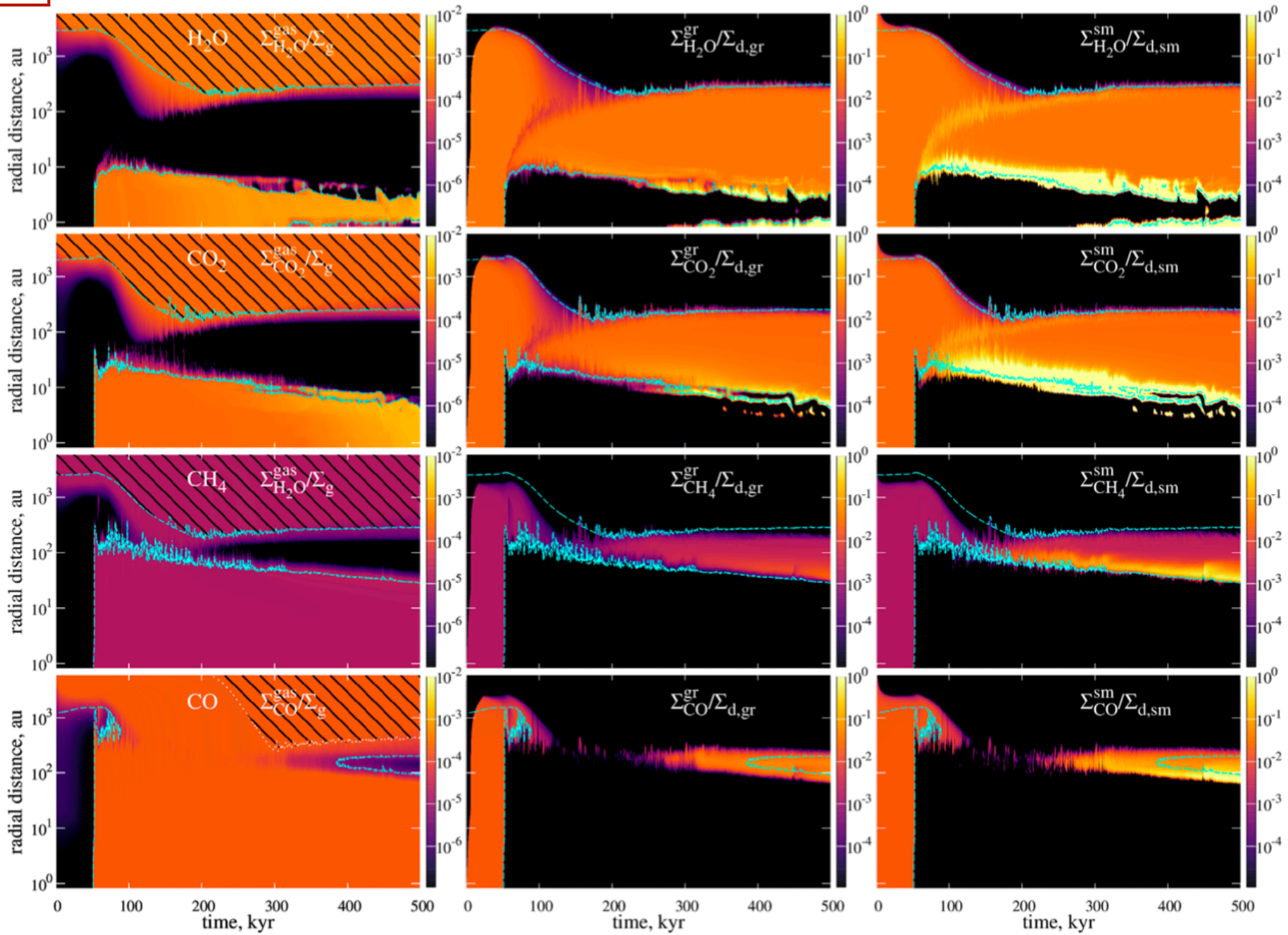

- 熱脱離で決まる内側のスノーラインと光脱離で決まる外側のスノーラインが存在
- 内側のスノーラインは時間と共に内側に移動
- 気相・固相共に、スノーラインで揮発性分子の存在量がピークを持つ

- スパイラルがある、円盤温度およびダスト分布がスパイラルに沿って変化するため、スノーラインもスパイラル状になる

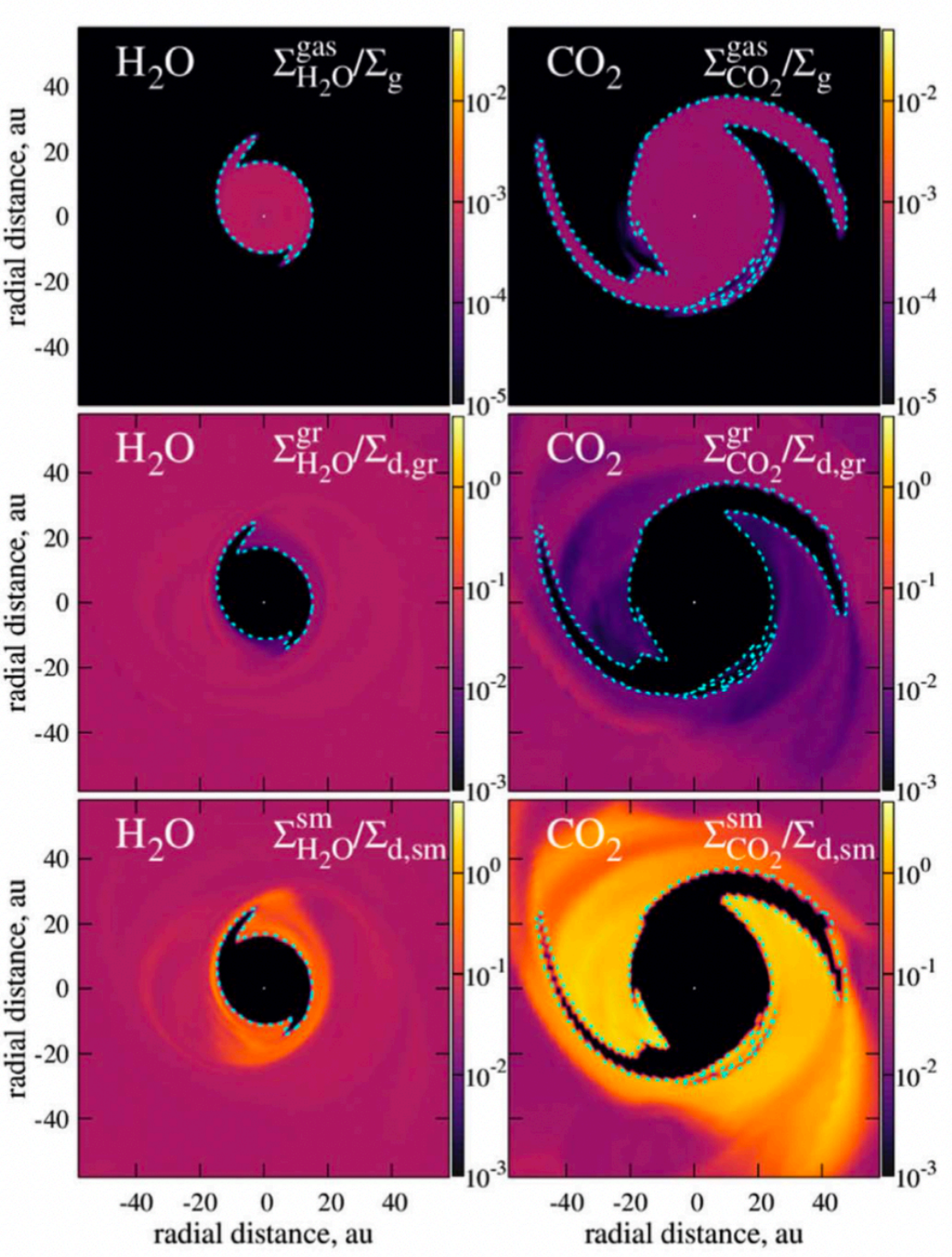

- 大きいダストのice/rock比は初期とほとんど変わらない ->大きいダストへのiceの凝縮は殆ど起きない

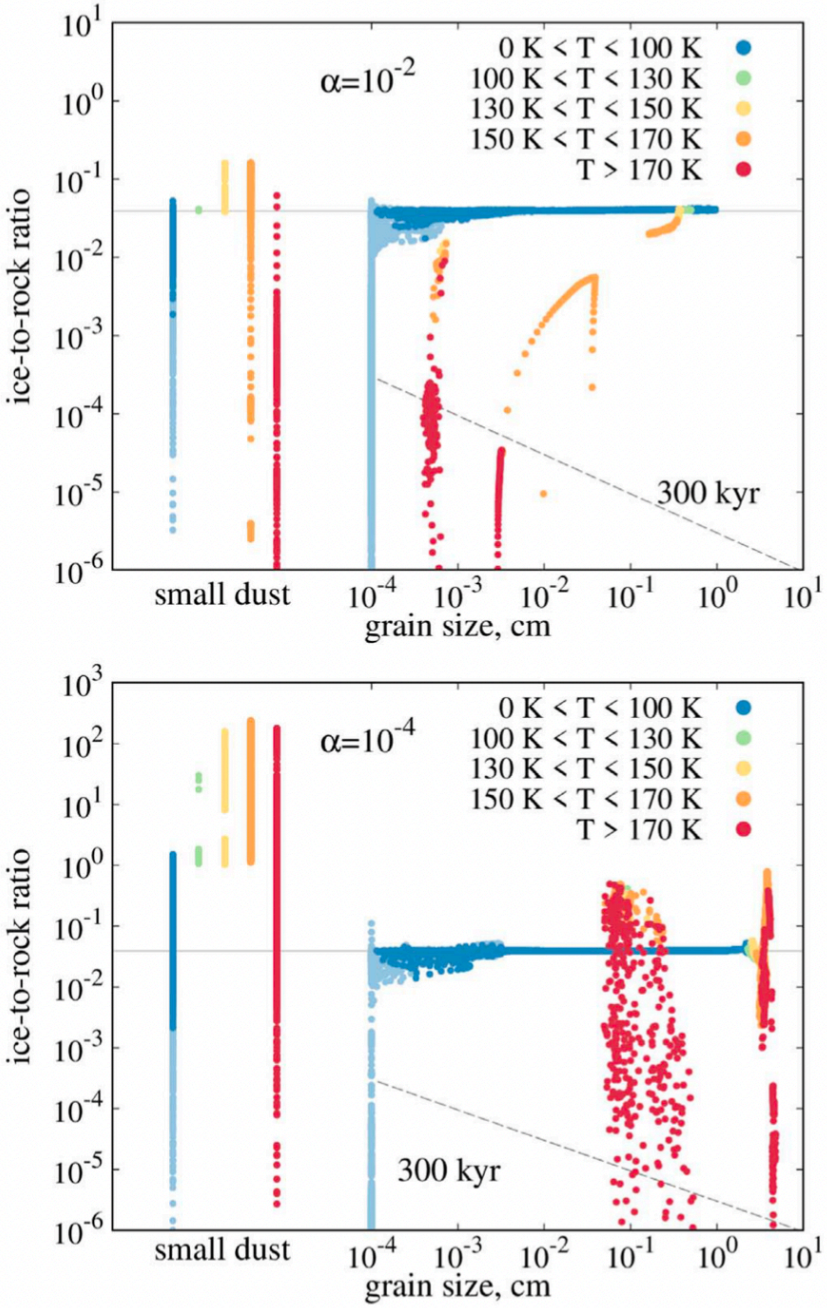

25. **Molecular Clouds in the Second Quadrant of the Milky Way Mid-plane from l=104.°75 to l=119.°75 and b=−5.°25 to b=5.°25**

Yuehui Ma, Hongchi Wang, Chong Li, Lianghao Lin, Yan Sun, Ji Yang ★ We have studied the properties of molecular clouds in the second quadrant of the Milky Way Mid-plane from l=104.°75 to l=119.°75 and b= −5.°25 to b=5.°25 using the ^{12}CO, ^{13}CO, and C^{18}O $J = 1-0$ emission line data from the Milky Way Imaging Scroll Painting project (MWISP). We have identified 857 and 300 clouds in the ^{12}CO and ^{13}CO spectral cubes, respectively, using the DENDROGRAM + SCIMES algorithms. The distances of the molecular clouds are estimated and the physical properties like masses, sizes, and surface densities of the clouds are tabulated. The molecular clouds in the Perseus arm are about 30−50 times more massive and 4−6 times larger than the clouds in the Local arm. This result, however, is likely biased by distance selection effects. The surface densities of the clouds are enhanced in the Perseus arm with an average value of ∼100 $M_\odot$ pc^{-2}. We selected the 40 most extended (>0.35 arcdeg^2) molecular clouds from the ^{12}CO catalog to build the H_2 column density probability distribution function (N-PDF). About 78% of the N-PDFs of the selected molecular clouds are well fitted with log-normal functions with only small deviations at high-densities which correspond to star-forming regions with scales of ∼1-5 pc in the Local arm and ∼5-10 pc in the Perseus arm. About 18% of the selected molecular clouds have power-law N-PDFs at high-densities. In these molecular clouds, the majority of the regions fitted with the power-law correspond to molecular clumps of sizes of ∼1 pc or filaments of widths of ∼1 pc.

https://arxiv.org/abs/2102.12199

26. **The Galactic HII Region Luminosity Function at Radio and Infrared Wavelengths**

J. L. Mascoop, L. D. Anderson, Trey. V. Wenger, Z. Makai, W. P. Armentrout, Dana. S. Balser, T. M. Bania ★ The Galactic HII region luminosity function (LF) is an important metric for understanding global star formation properties of the Milky Way, but only a few studies have been done and all use relatively small numbers of HII regions. We use a sample of 797 first Galactic quadrant HII regions compiled from the WISE Catalog of Galactic HII Regions to examine the form of the LF at multiple infrared and radio wavelengths. Our sample is statistically complete for all regions powered by single stars of type O9.5V and earlier. We fit the LF at each wavelength with single and double power laws. Averaging the results from all wavelengths, the mean of the best-fit single power law index is $\langle\alpha\rangle = -1.75 \pm 0.01$. The mean best-fit double power law indices are $\langle\alpha_1\rangle = -1.40 \pm 0.03$ and $\langle\alpha_2\rangle = -2.33 \pm 0.04$. We conclude that neither a single nor a double power law is strongly favored over the other. The LFs show some variation when we separate the HII region sample into subsets by heliocentric distance, physical size, Galactocentric radius, and location relative to the spiral arms, but blending individual HII regions into larger complexes does not change the value of the power law indices of the best-fit LF models. The consistency of the power law indices across multiple wavelengths suggests that the LF is independent of wavelength. This implies that infrared and radio tracers can be employed in place of Hα.

https://arxiv.org/abs/2102.09033

28. **Dipper-like variability of the Gaia alerted young star V555 Ori**

Zsófia Nagy, Elza Szegedi-Elek, Péter Ábrahám, Ágnes Kóspál, Attila Bódi, Jérôme Bouvier, Mária Kun, Attila Moór, Borbála Cseh, Anikó Farkas-Takács, Ottó Hanyecz, Simon Hodgkin, Bernadett Ignácz, Réka Könyves-Tóth, Levente Kriskovics, Gábor Marton, László Mészáros, András Ordasi, András Pál, Paula Sarkis, Krisztián Sárneczky, Ádám Sódor, Zsófia Marianna Szabó, Róbert Szakáts, Dóra Tarczay-Nehéz, Krisztián Vida, Gabriella Zsidi

★ V555 Ori is a T Tauri star, whose 1.5 mag brightening was published as a Gaia science alert in 2017. We carried out optical and near-infrared photometric, and optical spectroscopic observations to understand the light variations. The light curves show that V555 Ori was faint before 2017, entered a high state for about a year, and returned to the faint state by mid-2018. In addition to the long-term flux evolution, quasi-periodic brightness oscillations were also evident, with a period of about 5 days. At optical wavelengths both the long-term and short-term variations exhibited colourless changes, while in the near-infrared they were consistent with changing extinction. We explain the brightness variations as the consequence of changing extinction. The object has a low accretion rate whose variation in itself would not be enough to reproduce the optical flux changes. This behaviour makes V555 Ori similar to the pre-main sequence star AA Tau, where the light changes are interpreted as periodic eclipses of the star by a rotating inner disc warp. The brightness maximum of V555 Ori was a moderately obscured (A_V=2.3 mag) state, while the extinction in the low state was A_V=6.4 mag. We found that while the Gaia alert hinted at an accretion burst, V555 Ori is a standard dipper, similar to the prototype AA Tau. However, unlike in AA Tau, the periodic behaviour was also detectable in the faint phase, implying that the inner disc warp remained stable in both the high and low states of the system.

https://arxiv.org/abs/2103.10313

30. **The substructure of the Perseus star forming region: A survey with Gaia DR2**

Tatiana Pavlidou, Aleks Scholz, Paula S. Teixeira

★ We use photometric and kinematic data from Gaia DR2 to explore the structure of the star forming region associated with the molecular cloud of Perseus. Apart from the two well known clusters, IC 348 and NGC 1333, we present five new clustered groups of young stars, which contain between 30 and 300 members, named Autochthe, Alcaeus, Heleus, Electryon and Mestor. We demonstrate these are co-moving groups of young stars, based on how the candidate members are distributed in position, proper motion, parallax and colour-magnitude space. By comparing their colour-magnitude diagrams to isochrones we show that they have ages between 1 and 5 Myr. Using 2MASS and WISE colours we find that the fraction of stars with discs in each group ranges from 10 to 50 percent. The youngest of the new groups is also associated with a reservoir of cold dust, according to the Planck map at 353 GHz. We compare the ages and proper motions of the five new groups to those of IC 348 and NGC 1333. Autochthe is clearly linked with NGC 1333 and may have formed in the same star formation event. The seven groups separate roughly into two sets which share proper motion, parallax and age: Heleus, Electryon, Mestor as the older set, and NGC 1333, Autochthe as the younger set. Alcaeus is kinematically related to the younger set, but at a more advanced age, while the properties of IC 348 overlap with both sets. All older groups in this star forming region are located at higher galactic latitude.

https://arxiv.org/abs/2102.08263

31. Detection of new O-type stars in the obscured stellar cluster Tr 16-SE in the Carina Nebula with KMOS

Thomas Preibisch, Stefan Flaischlen, Christiane Göppl, Barbara Ercolano, Veronica Roccatagliata ★ The Carina Nebula harbors a large population of high-mass stars, including at least 75 O-type and Wolf-Rayet stars, but the current census is not complete since further high-mass stars may be hidden in or behind the dense dark clouds that pervade the association. With the aim of identifying optically obscured O- and early B-type stars in the Carina Nebula, we performed the first infrared spectroscopic study of stars in the optically obscured stellar cluster Tr 16-SE, located behind a dark dust lane south of eta Car. We used the integral-field spectrograph KMOS at the ESO VLT to obtain H- and K-band spectra with a resolution of R sim 4000 (Delta lambda sim 5 A) for 45 out of the 47 possible OB candidate stars in Tr 16-SE, and we derived spectral types for these stars. We find 15 stars in Tr 16-SE with spectral types between O5 and B2 (i.e., high-mass stars with M >= 8 Msun, only two of which were known before. An additional nine stars are classified as (Ae)Be stars (i.e., intermediate-mass pre-main-sequence stars), and most of the remaining targets show clear signatures of being late-type stars and are thus most likely foreground stars or background giants unrelated to the Carina Nebula. Our estimates of the stellar luminosities suggest that nine of the 15 O- and early B-type stars are members of Tr 16-SE, whereas the other six seem to be background objects. Our study increases the number of spectroscopically identified high-mass stars (M >= 8 Msun) in Tr 16-SE from two to nine and shows that Tr 16-SE is one of the larger clusters in the Carina Nebula. Our identification of three new stars with spectral types between O5 and O7 and four new stars with spectral types O9 to B1 significantly increases the number of spectroscopically identified O-type stars in the Carina Nebula.

https://arxiv.org/abs/2103.00196

32. A Galactic survey of radio jets from massive protostars

S. J. D. Purser, S. L. Lumsden, M. G. Hoare, S. Kurtz ★ In conjunction with a previous southern-hemisphere work, we present the largest radio survey of jets from massive protostars to date with high-resolution, ($\sim 0.04''$) VLA observations towards two subsamples of massive star-forming regions of different evolutionary statuses: 48 infrared-bright, massive YSOs and 8 IRDCs containing 16 luminous ($L_{bol} > 10^3\,L_\odot$) cores. For 94% of the MYSO sample we detect thermal radio ($\alpha \geq -0.1$ whereby $S_\nu \propto \nu^\alpha$) sources coincident with the protostar, of which 84% (13 jets and 25 candidates) are jet-like. Radio luminosity is found to scale with L_{bol} similarly to the low-mass case supporting a common mechanism for jet production across all masses. Associated radio lobes tracing shocks are seen towards 52% of jet-like objects and are preferentially detected towards jets of higher radio and bolometric luminosities, resulting from our sensitivity limitations. We find jet mass loss rate scales with bolometric luminosity as $\dot{m}_{jet} \propto {L_{bol}}^{0.9\pm0.2}$, thereby discarding radiative, line-driving mechanisms as the dominant jet-launching process. Calculated momenta show that the majority of jets are mechanically capable of driving the massive, molecular outflow phenomena since $p_{jet} > p_{outflow}$. Finally, from their physical extent we show that the radio emission can not originate from small, optically-thick HII regions. Towards the IRDC cores, we observe increasing incidence rates/radio fluxes with age using the proxy of increasing luminosity-to-mass $\left(\frac{L}{M}\right)$ and decreasing infrared flux ratios $\left(\frac{S_{70\mu m}}{S_{24\mu m}}\right)$. Cores with $\frac{L}{M} < 40\,L_{sol}{M_{sol}}^{-1}$ are not detected above (5.8GHz) radio luminosities of $\sim 1 mJy\,kpc^2$.

https://arxiv.org/abs/2103.08990